THE JOURNAL OF PHYSICAL CHEMISTRY B

ARTICLE

pubs.acs.org/JPCB

Charge Transport Properties of Stacking Bisindenoanthrazolines: DFT Studies

Hongguang Liu,[†] Jinglin Mu,[‡] and Jin Yong Lee*[,†,§]

[†]Department of Chemistry, Sungkyunkwan University, Suwon 440-746, Korea

[‡]Key Laboratory of Colloid and Interface Chemistry, Ministry of Education, Institute of Theoretical Chemistry, Shandong University, Jinan 250100, P. R. China

[§]Supercomputing Center, Korea Institute of Science and Technology Information, Yuseong, Daejeon 305-806, Korea

Supporting Information

ABSTRACT: Organic semiconductors to date having cofacial stacking motif are scarce compared to those having herringbone motif. Recently, Ahmed and co-workers have reported a series of novel n-type bisindenoanthrazolines (BIDAs) [*Chem. Mater.* **2010**, *22*, 5786], among which DADF and DADK adopt different slipped cofacial arrangements exhibiting distinct electron transport abilities. Here, we performed computational studies to understand the relationship between charge transport and molecular packing for these BIDAs molecules. This work focuses on the intrinsic molecular factors required for efficient and long-range charge transfer. Unlike the previous studies only focusing the charge injection barriers or the carrier mobilities, herein, we present the notion that lower electron injection barrier and higher intrinsic electron mobility should be both satisfied to achieve better n-type OFETs. We also note that the actual mobility can be significantly underestimated due to the limitation of the space-charge limited current method. Through computational modeling, we rationalized the superior electron conductivity of DADK and also shed light on the favorable or undesirable properties for efficient charge transport of BIDAs. Another key finding is that the intrinsic electron and hole mobilities are quite deviated from each other rather than comparable in current mobility calculations.

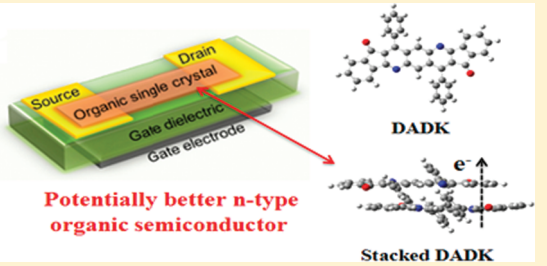

INTRODUCTION

Organic semiconductors are of enormous current interest, not only for the vast applications they offer, including organic photovoltaic (OPV) cells,[1] organic electrochromic devices (ECDs),[2] organic light-emitting diodes (OLEDs),[3] and organic field-effect transistors (OFETs),[4] but also for the intrinsic scientific challenges they present, such as controllable single crystal growth, promoted device fabrication, suitable materials with good air-stability, and higher charge transport efficiency. From both a fundamental and practical point of view, understanding the relationship between charge transport and molecular packing in crystals is essential and provides both chemists and physicists with rules to design optimum devices.

Among the most popular organic semiconductors, polycyclic heteroarenes[5] attract many scientists due to their planar backbone frameworks; a primary delocalization induced by π-conjugation is established within the molecular plane. Improved intermolecular interactions allow for a secondary delocalization along the packing direction due to the overlap of intermolecular π-orbitals providing charge transport pathways through the molecule stacks. Over the past decades, a lot of efforts have been dedicated to developing p-type (hole-transporting) organic semiconductors.[6] Some famous representatives, like pentacene,[7] rubrene,[8] fused oligothiophenes,[5b,6b] and oligofluorenes,[9] present superior charge transport performance to amorphous silicon.[6a,10] Despite the fact that both p-type and n-type devices are required to create a low-power consumption complementary metal-oxide-semiconductor (CMOS),[11] there is a lack of organic semiconductors with comparable processing and performance for n-type (electron-transporting) OFETs.[12,13]

For designing n-type organic semiconductors, a commonly used strategy is the introduction of electron withdrawing groups such as fluorine,[11] imine nitrogens,[14] or carbonyls,[15] because these electron deficient moieties are believed to lower the LUMO energy level thus facilitating the electron injection from electrodes[11,16] and enhancing the air-stability of n-type materials.[15,17] More recently, instead of pursuing more appropriate electron withdrawing groups, several theoretical investigations have been done to rationalize the high sensitivity of the charge transport with respect to the relative positions of the interacting molecules. Brédas and co-workers have previously demonstrated, in a tetracene cofacial dimer, that even small molecular displacements can lead to a situation where the transfer integral for electrons are larger than for holes and hence where electrons can be possibly

Received: March 24, 2011
Revised: April 26, 2011
Published: June 13, 2011

ACS Publications © 2011 American Chemical Society

dx.doi.org/10.1021/jp202745w | *J. Phys. Chem. B* 2011, 115, 8409–8416

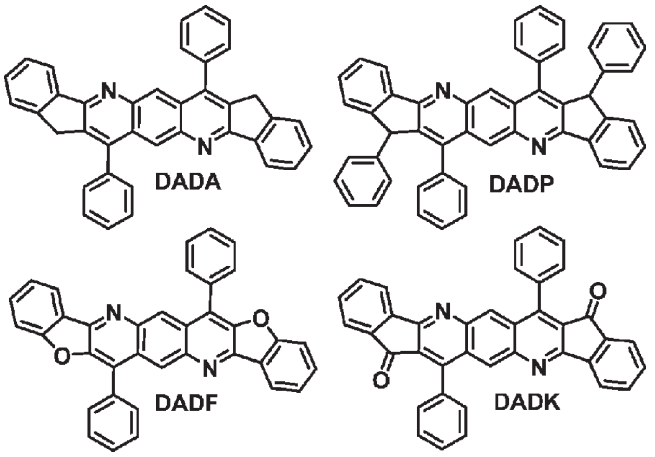

Figure 1. Molecular structures of bisindenoanthrazolines.[22]

more mobile than holes.[18] Besides, Marks and co-workers also reported for the slipped π-stacked arrangement of oligothiophenes that the computed hole transfer rate decreased significantly, and for the cofacial dimer, the calculated electron transfer rate was ~2 times greater than the hole transfer rate.[19] Our previous work on one-dimensional stacks of annelated β-trithiophenes also revealed that optimized cofacial geometry can lead to remarkably increased electron mobility.[20] Here, it is important to recall, in most cases, the characterization of a p-type or n-type organic semiconductor does not rely on the intrinsic ability of the material to transport holes or electrons; it rather reflects the ease of charge injection from electrodes used in devices.[18,21] However, as optimum conditions, both the lower electron injection barrier and higher electron transport mobility should be satisfied to achieve better n-type OFETs.

It is widely accepted that organic semiconductors must have suitable HOMO or LUMO energies to promote hole or electron injection from the source electrode and to optimize charge transport in the OFET channel as well as device air-stability.[17a] Much literature has demonstrated the close relationship between the HOMO energy level and ionization potential (IP) and the intimate connection between the LUMO energy level and electron affinity (EA).[21,22] For organic semiconductors, those parameters always play a crucial role in determining the charge transport characteristics and environmental stability. It was reported that lowering the energy of LUMO could enhance the air-stability of n-type materials.[17] Increased electron affinity by introducing an electron deficient group can reduce the sensitivity of mobile electrons to trap state[23] and suggests a good potential for electron transport, whereas a lower HOMO energy is generally an indicator of better air-stability in OFETs. Materials having large IP values are considered to be excellent for blocking holes in OLEDs.[22]

Ladder-type polycyclic aromatics incorporated with imine nitrogens are of immense current interest in the development of n-type semiconductors.[14,15,17a] The prominent advantages of these conjugated oligomers are that they have (i) lower LUMO energy level, (ii) enhanced electron affinity, (iii) increased propensity of π-stacking, and (iv) better photo-oxidative stability. More recently, a series of novel n-type bisindenoanthrazolines (BIDAs) have been reported by Ahmed et al.[22] Although the n-type performances of four BIDAs (DADA, DADP, DADF, and DADK) were far from satisfactory (the highest electron mobility was 3.84×10^{-4} cm^2 V^{-1} s^{-1} measured by the space-charge limited current (SCLC) method in ambient conditions), the crystal structures of DADF and DADK demonstrated distinct stacking modes. More specifically, DADF formed a parallel slipped π-stacking along the *b* axis and edge-to-face interactions in the (101) direction. DADK adopted an antiparallel slipped π-stacking along the *a* axis. This is interesting since the only difference between DADF and DADK molecules is the substituent (X = ether in DADF; X = carbonyl in DADK) as seen in Figure 1, and organic semiconductors to date having slipped cofacial stacking mode are scarce compared to those having herringbone mode.[4a,18] Several studies have focused on the electron transport along the stacking direction in π-stacked systems.[24] In addition, the observed low electron mobility was considered because of the limitation that the SCLC method used in that work measured the charge mobility along the direction perpendicular to the substrate, whereas the optimum direction for charge transport (π-stacking direction) was parallel to the substrate. In other words, the actual mobility of the major carrier could be dramatically underestimated. To verify this, we performed charge mobility calculations on six BIDAs dimers along the π-stacking direction. Moreover, the stacking-geometry-induced variations of charge transport properties were also systematically investigated.

COMPUTATIONAL METHODS

Density functional theory (DFT) has long been used to predict accurate bandwidths in solid-state materials, and some functionals like B3LYP have been proven to be accurate for calculating ionization potentials,[25] electron affinities,[25,26] orbital energies,[27] and molecular structures.[28] However, it is also known to describe weak interactions poorly, including van der Waals and $\pi-\pi$ interactions.[29] Conversely, the second-order Møller–Plesset perturbation theory (MP2) has received wide acceptance for accurately describing weak electrostatic and dispersive energetic interactions between organic π-dimers, such as thiophene and benzene,[30] but the MP2 method is rather computationally demanding and can rarely be applied to large molecular structures. Additionally, the orbital energies calculated by MP2 have been less frequently employed for bandwidths or orbital overlap.[31] In contrast to MP2, DFT has been successfully employed to investigate large molecules and large-scale systems due to its fast computational speed. In addition to the salient efficiency of the theory, DFT has been proven to be reasonably accurate for calculating the chemical and structural properties of species such as organic semiconductors and conventional inorganic semiconductors.[32] Among the tested hybrid meta DFT functionals, MPWB1K provides the best results for the combination of thermochemistry, thermochemical kinetics, hydrogen bonding, and weak interactions.[33] The MPWB1K functional also has been confirmed to be adequate for treating π-stacking, H-bonding interactions,[34] and CH/π interactions.[35] Hence, as a useful DFT method which provides the best performance in charge transfer interactions,[33b] MPWB1K is sufficient for evaluating the charge transport properties of the stacked BIDAs molecules.

Although Ahmed et al. failed to grow suitable single crystals of DADA and DADP for X-ray single-crystal diffraction, they expected these BIDAs shared a similar planar backbone structure with that of DADF and DADK, and they also predicted that DADA and DADP should have larger intermolecular distances than those in DADF and DADK. In this context, we first optimized the molecular structures of the four bisindenoanthrazolines

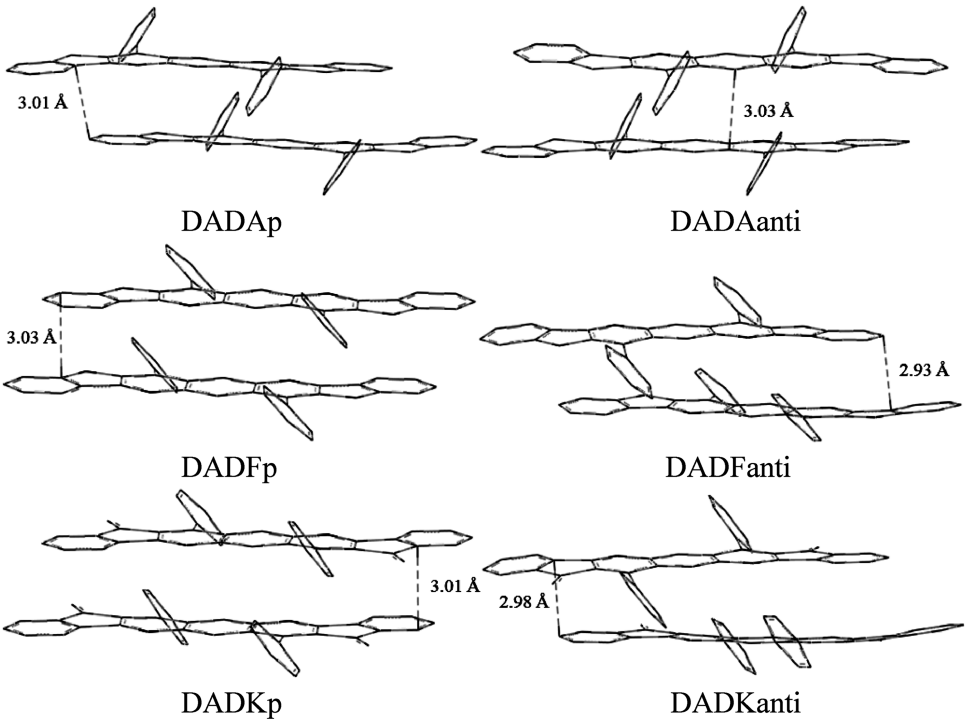

Figure 2. Molecular structures of the dimers (hydrogen atoms are deleted for clarity).

(DADA, DADP, DADF, and DADK), and we further established the BIDAs stacking dimers with parallel and antiparallel orientations, respectively, to investigate the stacking-geometry-induced charge transport characteristics. However, the design of DADP dimers with proper intermolecular separations was unsuccessful, because of the large steric hindrance between two neighboring molecules caused by the additional benzyl substituent. Therefore, a total of six BIDAs dimers (DADAp, DADFp, and DADKp for parallel stacks and DADAanti, DADFanti, and DADKanti for antiparallel stacks) were designed, and the shortest intermolecular separations were assigned within the typical π-stacking distance of 3.4−3.6 Å.[36] All of the structure optimizations were performed with MPWB1K in association with the 3-21G* basis sets, employing a suite of Gaussian 03 programs.[37] In addition, EA/IP was defined as $E(D_x^-)/E(D_x^+) - E(D_x)$, where $E(D_x^-)/E(D_x^+)$ and $E(D_x)$ denote the energies of anions/cations at the neutral optimized geometries and the neutral energy, respectively.

At room temperature, the charge migrations in the OFET can be correctly described as a hopping mechanism. The relationship of the carrier mobility μ and charge transfer rate k_{CT} can be obtained via the Einstein relation[38]

$$\mu = eL^2 k_{CT}/2k_B T \quad (1)$$

where e, L, k_B, and T correspond to the electronic charge, transport distance (approximated by the molecular center-to-center distance of a dimer), Boltzmann constant, and temperature. According to the semiclassical Marcus theory,[39] the charge transfer rate between two neighboring molecules can be expressed as

$$k_{CT} = \frac{4\pi^2}{h}\frac{1}{\sqrt{4\pi\lambda k_B T}}t^2 \exp\left(-\frac{\lambda}{4k_B T}\right) \quad (2)$$

Here, h is the Planck constant and t and λ correspond to the transfer integral and the internal reorganization energy, respectively. The total internal reorganization energy λ can be obtained as the sum of two relaxation energy terms: (i) the difference between the energies of the neutral molecule in its equilibrium geometry and in the relaxed geometry characteristic of the radical ion and (ii) the difference between the energies of the radical ion in its equilibrium geometry and in the neutral geometry. The absolute value of the transfer integral t for electron [hole] transport is approximated using the Koopmans' theorem,[40] relying on the one-electron approximation

$$t = \frac{E_{L+1[H]} - E_{L[H-1]}}{2} \quad (3)$$

where $E_{L[H]}$ and $E_{L+1[H-1]}$ are the energies of the LUMO [HOMO] and LUMO+1 [HOMO-1] in the closed-shell configuration of the neutral state, respectively. As is reported by Valeev et al.,[41] the value of t obtained by the energy-splitting approach is reliable, only when the dimer is symmetric; that is, the two localized valence structures $M_1^*-M_2$ and $M_1-M_2^*$ (* denotes the positive or negative charge) can be obtained from one another by a symmetric transformation. Otherwise, the transfer integral can be drastically overestimated, due to the neglect of polarization impacts on the site energies. Assuming that the dimer LUMO and LUMO+1 (HOMO and HOMO-1) result from the interaction of only monomer LUMOs (HOMOs), by applying Löwdin's symmetric transformation to the localized monomer orbitals,[42] the energy splitting in the orthogonal basis[41] is given by

$$E_{L+1[H]} - E_{L[H-1]} = \sqrt{(e_1^{eff} - e_2^{eff})^2 + (2t^{eff})^2} \quad (4)$$

Here, e_1^{eff} and e_2^{eff} are the site energies. Apparently, the transfer integral can be estimated as half of the splitting energy only when the site energy difference is zero. The errors arising from the energy-splitting approach can be avoided by calculating the transfer integrals directly, in terms of properly orthogonalized

dx.doi.org/10.1021/jp202745w |J. Phys. Chem. B 2011, 115, 8409–8416

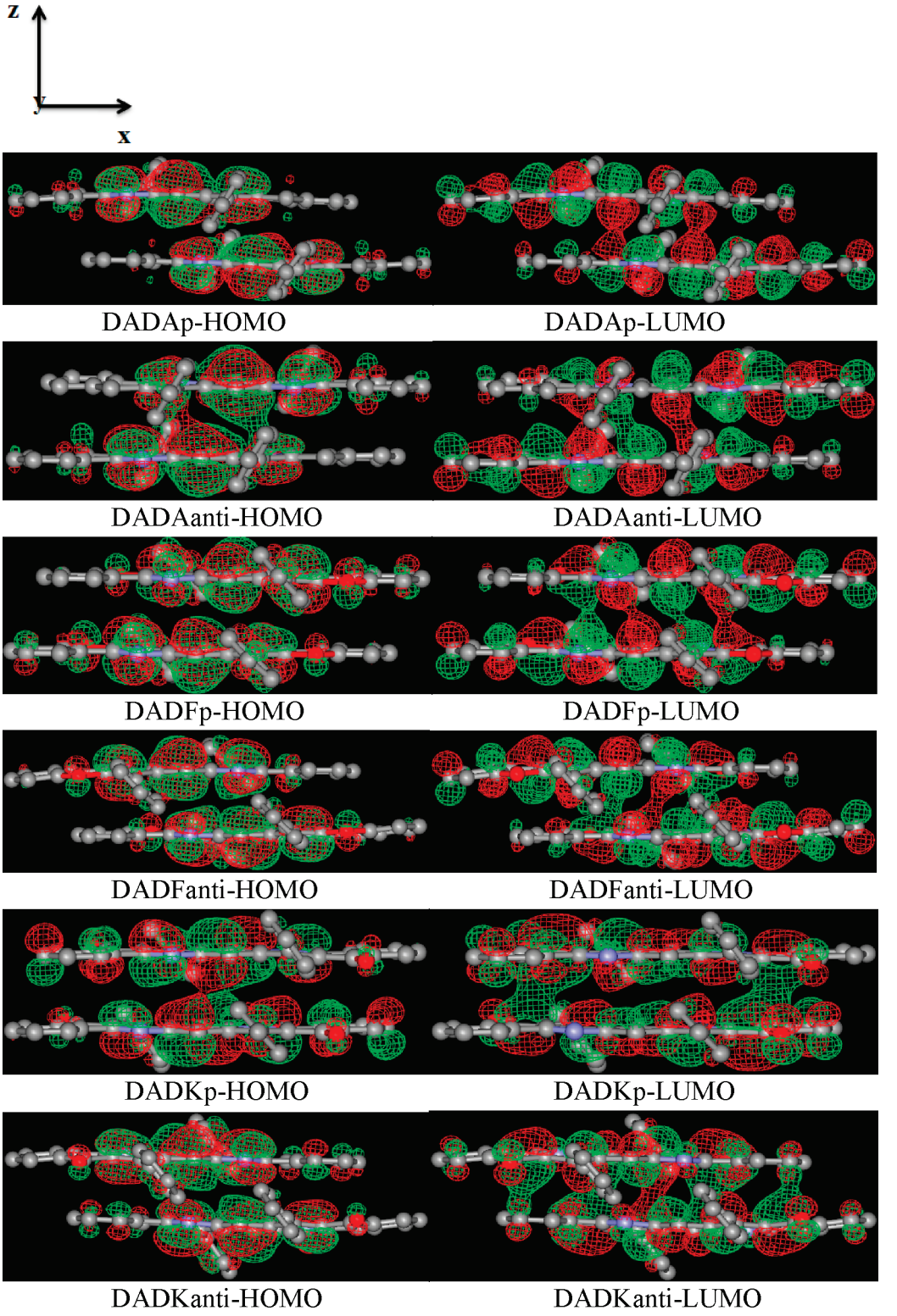

Figure 3. Highest occupied molecular orbitals (HOMO) and lowest unoccupied molecular orbitals (LUMO) of optimized BIDAs dimers. Hydrogen atoms are deleted for clarity. Internal Cartesian axes are shown, and the view down is the *y* axis.

monomer orbitals[41]

$$t^{\text{eff}} = \frac{t_{12} - \frac{1}{2}(e_1 + e_2)S_{12}}{1 - {S_{12}}^2} \qquad (5)$$

where t_{12}, e_1, and e_2 are matrix elements from the system Hamiltonian. S_{12} is the spatial overlap integral between the LUMOs (HOMOs) of the two monomers.

Herein, in order to evaluate the polarization caused by intermolecular interactions, we calculated and compared the

transfer integrals by eqs 3 and 5. Surprisingly, we found that the results were nearly identical, which indicated the polarization along the stacking direction was small and its impact on the site energy was limited. Therefore, the transfer integrals obtained by Koopmans' theorem were reliable in our stacking models. Detailed discussion regarding the polarization will be provided in the later text.

RESULTS AND DISCUSSION

The molecular packing diagram in Figure 2 demonstrates the optimized BIDAs dimers formed slipped face-to-face π-stacking modes. It was clear to see the series of BIDAs had a common framework of a planar heptacyclic ring that comprised an anthrazoline ring core with two imine nitrogens in the backbone. DADAanti is lower in energy than DADAp by 15.72 kcal/mol, whereas the energies of DADFp and DADKp are only slightly more stable than DADFanti and DADKanti by 0.74 and 1.77 kcal/mol, respectively. Thus, for DADF and DADK, both parallel and antiparallel geometries may be obtained in the experiment. The phenyl rings of DADKanti had a twist angle of 51° compared to 45° in the case of DADFp. This was similar to the trend in the crystal that the twist angle for DADK (68°) was larger than that of DADF (61°). The shortest intermolecular distance between two molecular backbones is displayed in Figure 2. Although the shortest intermolecular distance could not represent the average separation between two neighboring backbones (because the shortest intermolecular distance often occurred between the edge carbon atoms), it should be noted that these extremely short C···C contacts were rarely observed in the current π-stacking organic materials.[36] Several factors have been taken into account. First, since the dimers investigated here were extracted from the crystal periodic structures (or as a guide to construct a dimer which did not have a single crystal structure), the isolated dimers might not reflect the overall interactions in the crystal environment. In reality, the nearby "edge" molecules might serve as an electrostactic repulsion force that deviate the "face" molecules from closed stacking. Second, between adjacent molecules, the displacement along the long and/or short molecular axes could reduce the electrostatic repulsion terms,[18,19] and thus atoms at the molecular edge might become closer. Third, the dipole moment introduced by atoms or functional groups along a certain direction might stabilize the cofacial orientations,[12] and the antiparallel stacking minimized the steric hindrance, inducing a smaller intermolecular separation.

Knowledge of the molecular geometry as well as the frontier orbital characteristics is key to understand the charge transfer efficiency and majority carrier type. In this work, based on our computationally optimized models, we investigated the frontier orbital shapes, electronic couplings (orbital overlaps), and orbital energies. Figure 3 shows the highest occupied molecular orbitals (HOMOs) and the lowest unoccupied molecular orbitals (LUMOs) of six dimer candidates. For all candidate HOMOs, most electrons were localized over the central area of each monomer molecule, whereas some electrons were distributed over the terminal atoms. Since the HOMO wave functions are more related to hole transport,[16] the central spatial overlap area was believed to be responsible for hole migration. Compared to the HOMOs wave functions, the LUMOs patterns of BIDAs exhibited diffused electron distributions, and delocalization of the LUMO over the entire conjugated system suppressed the charge recombination, allowing for long-lived anion species and facilitating electron movement.[43] Thus, these strong interorbital overlaps in LUMOs suggested that bisindenoanthrazolines might be good candidates for n-type molecular electronic device materials because the LUMO wave functions are believed to be important for the electron transport. A close examination revealed that the strong interorbital overlaps resulted from the $\pi-\pi$ interactions between the BIDAs. It should be noted that DADKanti had the most extensive interorbital overlaps, indicating DADKanti was promising in making electronic devices with higher charge transfer ability. As is known, increased intermolecular overlap of electronic wave functions leads to increased bandwidth, which is directly related to carrier mobility in the coherent transport regime.[44] Also, from the standpoint of the hopping theory, charge mobility increases because the hopping rate increases with intermolecular orbital overlap.[39a,45] Since the only difference between each BIDA molecule was the substituents, therefore, the substituent oxygen atoms or carbonyl groups were considered to contribute substantially to the interorbital overlaps. The equilibrium structures also revealed that the phenyl rings on the para-position of N atoms were spatially and electronically isolated from the π orbitals. Isolation from the frontier orbitals minimized the electronic energetic effects of varying the twist angles of the phenyl groups, limiting their influence on crystal packing. The isolation also suggested a tolerance for sterically requiring phenyl groups without spatial intrusion into the $\pi-\pi$ stacking region. For each BIDA, the computed HOMO energy difference between antiparallel and parallel stacks was small (see Table 1), whereas the LUMO energy for antiparallel stack was lower than that of the parallel stack. The values of the HOMO level ranging from 5.87 to 6.63 eV were lower than those of most polythiophenes and pentacene,[7a] indicating a higher oxidative stability. It was worthy of notice that, among the BIDAs, DADK had the lowest frontier orbital energies, which suggested the best air-stability.

In order to obtain more insight into the stacking effects of BIDAs molecules, we compared the frontier orbital energy, HOMO−LUMO gap, ionization potential, and electron affinity in monomer (Table 2) and dimer (Table 1) geometries. As seen in Table 2, similar to the case in dimer structures, mDADK had

Table 1. Calculated Frontier Orbital Energies, HOMO-LUMO Gaps, Ionization Potentials, and Electron Affinities for BIDAs Monomers

	DADAp	DADAanti	DADFp	DADFanti	DADKp	DADKanti
HOMO (eV)	−5.87	−6.02	−5.92	−5.87	−6.63	−6.60
LUMO (ev)	−1.38	−1.43	−1.62	−1.78	−2.14	−2.36
H-L gap (eV)	4.49	4.59	4.30	4.09	4.49	4.24
IP (eV)	6.38	6.52	6.45	6.38	7.15	7.11
EA (eV)	−0.85	−0.89	−1.08	−1.25	−1.59	−1.81

Table 2. Calculated Frontier Orbital Energies, HOMO-LUMO Gaps, Ionization Potentials, and Electron Affinities for BIDAs Dimers

	mDADA	mDADP	mDADF	mDADK
HOMO (eV)	−6.32	−6.36	−6.26	−6.90
LUMO (eV)	−1.40	−1.41	−1.78	−2.08
H-L gap (eV)	4.92	4.95	4.48	4.82
IP (eV)	6.97	6.97	6.92	7.56
EA (eV)	−0.74	−0.81	−1.11	−1.42

dx.doi.org/10.1021/jp202745w |J. Phys. Chem. B 2011, 115, 8409–8416

Table 3. Charge Transport Parameters of BIDAs Dimers

	t^a (eV)	$t^{a,c}$(eV)	λ^a (eV)	k^a (s^{-1})	μ^a [$cm^2/(Vs)$]	t^b (eV)	$t^{b,c}$ (eV)	λ^b (eV)	k^b (s^{-1})	μ^b [$cm^2/(Vs)$]
DADAp	0.17	0.19	0.34	3.08×10^{13}	1.32	0.15	0.15	0.26	6.29×10^{13}	2.69
DADAanti	0.14	0.12	0.38	1.30×10^{13}	0.27	0.10	0.09	0.29	1.73×10^{13}	0.36
DADFp	0.08	0.08	0.33	6.55×10^{12}	0.15	0.02	0.02	0.39	3.16×10^{11}	0.007
DADFanti	0.17	0.17	0.28	5.73×10^{13}	2.07	0.11	0.08	0.23	4.52×10^{13}	1.63
DADKp	0.002	0.004	0.61	2.11×10^{8}	5×10^{-6}	0.08	0.05	0.33	7.10×10^{12}	0.16
DADKanti	0.07	0.05	0.29	8.97×10^{12}	0.32	0.25	0.28	0.25	1.94×10^{14}	6.94

[a] Parameters for hole. [b] Parameters for electron. [c] Transfer integrals obtained by eq 5.

the lowest frontier orbital energies among the four monomers. When changing the geometry from monomer (referring to monomers except mDADP) to dimer, the HOMOs energy levels increased with a magnitude around 0.3 eV. Although the variations of LUMOs levels were quite special, the dimerization effect seemed to have little influence on the LUMO energy level for mDADA. However, for mDADF and mDADK, only the stacking motif which was the same as that in the real crystal exhibited a notable impact on LUMO energy level; that is, the parallel stacking for mDADF increased the LUMO energy level, whereas the antiparallel stacking for mDADK decreased the level. The introductions of electron deficient moieties were shown to lower the LUMO energy level thus facilitating the electron injection from electrodes and eventually enhancing the electron conductivity. DADKanti displayed a good potential for n-type material, because the calculated energy barrier for charge injection from Al ($\Phi = -4.3$ eV)[46] was 1.94 eV for electron and 2.30 eV for hole, indicating a smaller injection barrier for electron transport, whereas for DADFp, the calculated injection barrier for electron (2.68 eV) was larger than that for hole (1.62 eV). Since DADK and DADF semiconductors were proven to be n-type, this might be due to the fact that, in DADF crystal, besides the π-stacking periodic structures, there also existed edge-to-face interactions in the (101) direction which might significantly influence the charge injection barrier at the interface. It was not surprising that the dimers had a smaller HOMO−LUMO gap than that of the monomers, because generally, the aggregated system gives a smaller energy gap. When looking into the IP and EA values, the electron deficient substituents evidently increased the absolute value of EA. It was also found that IP had a close connection with the HOMO energy level; that is, when the HOMO energy level decreased, the IP value increased. A similar connection was also observed between EA and LUMO energy level; that is, when the LUMO energy level decreased, the absolute value of EA became larger. As we cofacially stacked another layer on the monomer, the IP reduced significantly, while the absolute value of EA enhanced except for DADFp. Obviously, parallel stacking showed a small impact on the EA of DADF. It was reported that increased electron affinity reduced the sensitivity of mobile electrons to trap states and decreased LUMO energy could provide more charge carrier stabilization.[12]

Table 3 lists the charge transport parameters based on theoretical calculations of the BIDAs dimers. We presumed the charge transfer between each stacking molecule was governed by the hopping mechanism. Since the polarization along the z axis (stacking direction) might significantly influence the transfer integral by affecting the charge site energy, the transfer integral obtained by eq 3 might not be reliable due to the neglect of polarization. To this end, following the work of Siebbeles et al.[47]

Table 4. Calculated Systems Dipole Moments along each Cartesian Axis

	dipole moments (Debye)		
	x	y	z
DADAp	−0.0198	−0.0683	0.0092
DADAanti	0.0127	0.0334	0.0220
DADFp	−0.0022	−0.0012	0.0024
DADFanti	−0.0093	0.3485	−0.0099
DADKp	0.0001	0.0000	0.0001
DADKanti	0.0585	0.9682	−0.0405

and Valeev et al.,[41] we computed the transfer integral explicitly incorporating the polarization factors as well. As seen in Table 3, the transfer integrals calculated by eq 5 did not show a distinct difference compared to the results obtained by eq 3. In order to confirm this, the energies for the charge on each monomer site of a dimer (site energies) were also computed. The site energy difference was nearly zero for all six dimers (see Table S1 in the Supporting Information). This clearly indicated, for both parallel and antiparallel stacking dimers, the polarization along the z axis was negligible. The energy-splitting approach could still accurately predict the transfer integrals for the antiparallel dimers, even though the dimers were not symmetric because $M_1^*-M_2$ and $M_1-M_2^*$ could not be obtained from one another by a symmetric transformation. In Table 3, DADKanti showed the highest intrinsic electron transfer rate and mobility, due to the fact that DADKanti had a relatively small reorganization energy (0.25 eV) and the largest transfer integral (0.25 eV) for electron. This was not surprising, because DADKanti had the most extensive interorbital overlaps. On the contrary, DADKanti exhibited a poor ability to transport hole, resulting from the much smaller transfer integral (0.07 eV) for hole. Combining the previous discussion about the charge injection barrier for DADKanti, DADKanti displayed a lower injection barrier for electron and demonstrated that as a repeat unit in the crystal it was promising to act as n-type material, whereas in the case of DADFp, the intrinsic electron transfer rate and mobility showed smaller values, since DADFp had a smaller transfer integral (0.02 eV) and larger reorganization energy (0.39 eV) for electron than that for hole. It was worth noticing that DADKp displayed a considerably smaller value in the transfer integral and a larger value in the reorganization energy for hole, which might result from the high sensitivity of the charge transport parameters with respect to the relative positions of the interacting monomers[18] as well as the electronic repulsion induced by the carbonyl groups. Compared to DADKp and DADFp, the antiparallel geometry not only enhanced the transfer integral but also decreased the

reorganization energy, which might be explained by the minimization of the electronic repulsion caused by the electron withdrawing moieties and phenyl groups. Unlike previous literature which reported the intrinsic electron and hole mobilities were expected to be comparable in many organic semiconductors,[19,44b,48] our results revealed that the electron and hole mobilities could be significantly deviated and controlled by proper design.

In order to confirm the polarization within our models, we investigated the dipole moments as well. As evidenced in Table 4, the polarization along the z (charge transfer direction) and x axes was very small compared with that along the y axis. However, the dipole moments of DADFanti and DADKanti oriented toward the y axis were significantly higher than those in the other two directions. Such distinctions might be attributed to the interlaced distribution of electron deficient moieties, and phenyl groups were also found to play an important role in tuning the internal dipole moments (see Table S2 in the Supporting Information). It is important to remember that the SCLC method used in Ahmed's work measured the charge mobility along the y axis. The electron mobility could be drastically underestimated due to following reasons: (i) the optimum direction for charge transport should be along the z axis (π-stacking direction) rather than y axis and (ii) similar to the electric field effect,[49] polarization along the charge transfer direction was seen to reduce mobility.

CONCLUSIONS

This work provides a theoretical point of view for understanding the relationship between charge transport and molecular packing for the novel n-type bisindenoanthrazolines semiconductors. Unlike the previous studies, which only focused on the charge injection barriers or the carrier mobilities, herein, we present the notion that higher intrinsic electron mobility and lower electron injection barrier should both be satisfied to achieve better n-type OFETs. We also note that the actual mobility can be significantly underestimated due to the limitations of the SCLC method. Through computational modeling, we rationalized the superior electron conducting ability of DADK and also shed light on the favorable or undesirable properties for efficient charge transport of BIDAs. Another important finding is that the intrinsic electron and hole mobility can be deviated rather than comparable in current mobility calculations. Our work is helpful in evaluating structural modification options and realizing better charge transfer efficiency.

ASSOCIATED CONTENT

Supporting Information. Optimized structures of BIDAs monomers, calculated site energies, and molecular dipole moments without the phenyl group. This material is available free of charge via the Internet at http://pubs.acs.org.

AUTHOR INFORMATION

Corresponding Author
*Phone: +82-31-299-4560. Fax: +82-31-290-7075. E-mail: jinylee@skku.edu.

ACKNOWLEDGMENT

This work was supported by the National Research Foundation (NRF) Grant (2010-0001630) funded by MEST.

REFERENCES

(1) (a) Cheng, Y. J.; Yang, S. H.; Hsu, C. S. *Chem. Rev.* **2009**, *109*, 5868. (b) Thompson, B. C.; Fréchet, J. M. J. *Angew. Chem., Int. Ed.* **2008**, *47*, 58.

(2) (a) Argun, A. A.; Aubert, P. H.; Thompson, B. C.; Schwendeman, I.; Gaupp, C. L.; Hwang, J.; Pinto, N. J.; Tanner, D. B.; MacDiarmid, A. G.; Reynolds, J. R. *Chem. Mater.* **2004**, *16*, 4401. (b) Beaujuge, P. M.; Reynolds, J. R. *Chem. Rev.* **2010**, *110*, 268.

(3) (a) Friend, R. H.; Gymer, R. W.; Holmes, A. B.; Burroughs, J. H.; Marks, R. N.; Taliani, C.; Bradly, D. D. C.; Dos Santos, D. A.; Brédas, J. L.; Lögdlund, M.; Salaneck, W. R. *Nature* **1999**, *397*, 121. (b) Shirota, Y.; Kageyama, H. *Chem. Rev.* **2007**, *107*, 953.

(4) (a) Zaumseil, J.; Sirringhaus, H. *Chem. Rev.* **2007**, *107*, 1296. (b) Wen, Y.; Liu, Y. *Adv. Mater.* **2010**, *22*, 1331.

(5) (a) Jones, B. A.; Ahrens, M. J.; Yoon, M. H.; Facchetti, A.; Marks, T. J.; Wasielewski, M. R. *Angew. Chem., Int. Ed.* **2004**, *43*, 6363. (b) Gao, P.; Beckmann, D.; Tsao, H. N.; Feng, X.; Enkelmann, V.; Baumgarten, M.; Pisula, W.; Müllen, K. *Adv. Mater.* **2009**, *21*, 213. (c) Tonzola, C. J.; Kulkarni, A. P.; Gifford, A. P.; Kaminsky, W.; Jenekhe, S. A. *Adv. Funct. Mater.* **2007**, *17*, 863.

(6) (a) Anthony, J. E. *Chem. Rev.* **2006**, *106*, 5028. (b) Gao, P.; Feng, X.; Yang, X.; Enkelmann, V.; Baumgarten, M.; Müllen, K. *J. Org. Chem.* **2008**, *73*, 9207. (c) Guo, Y.; Zhao, H.; Yu, G.; Di, C. A.; Liu, W.; Jiang, S.; Yan, S.; Wang, C.; Zhang, H.; Sun, X.; Tao, X.; Liu, Y. *Adv. Mater.* **2008**, *20*, 4835. (d) Katz, H. E.; Bao, Z. N.; Gilat, S. L. *Acc. Chem. Res.* **2001**, *34*, 359.

(7) (a) Xiao, K.; Liu, Y. Q.; Qi, T.; Zhang, W.; Wang, F.; Gao, J. H.; Qiu, W. F.; Ma, Y. Q.; Cui, G. L.; Chen, S. Y.; Zhan, X. W.; Yu, G.; Qin, J. G.; Hu, W. P.; Zhu, D. B. *J. Am. Chem. Soc.* **2005**, *127*, 13281. (b) Kim, K.; Yoon, Y. K.; Mun, M. O.; Park, S. P.; Kim, S. S.; Im, S.; Kim, J. H. *J. Supercond.* **2002**, *15*, 595. (c) Boronat, M.; Viruela, R.; Orti, E. *Synth. Met.* **1995**, *71*, 2291.

(8) (a) Menard, E.; Marchenko, A.; Podzorov, V.; Gershenson, M. E.; Fichou, D.; Rogers, J. A. *Adv. Mater.* **2006**, *18*, 1552. (b) Nakayama, K.; Hara, K.; Tominari, Y.; Yamagishi, M.; Takeya, J. *Appl. Phys. Lett.* **2008**, 93.

(9) (a) Yang, C.; Scheiber, H.; List, E. J. W.; Jacob, J.; Müllen, K. *Macromolecules* **2006**, *39*, 5213. (b) Zhou, Y.; Liu, W. J.; Ma, Y.; Wang, H.; Qi, L.; Cao, Y.; Wang, J.; Pei, J. *J. Am. Chem. Soc.* **2007**, *129*, 12386.

(10) Tang, M. L.; Reichardt, A. D.; Miyaki, N.; Stoltenberg, R. M.; Bao, Z. *J. Am. Chem. Soc.* **2008**, *130*, 6064.

(11) (a) Newman, C. R.; Frisbie, C. D.; da Silva, D. A.; Brédas, J. L.; Ewbank, P. C.; Mann, K. R. *Chem. Mater.* **2004**, *16*, 4436. (b) Bao, Z. N.; Rogers, J. A.; Katz, H. E. *J. Mater. Chem.* **1999**, *9*, 1895.

(12) (a) Ie, Y.; Nitani, M.; Ishikawa, M.; Nakayama, K.; Tada, H.; Kaneda, T.; Aso, Y. *Org. Lett.* **2007**, *9*, 2115. (b) Ie, Y.; Umemoto, Y.; Okabe, M.; Kusunoki, T.; Nakayama, K. I.; Pu, Y. J.; Kido, J.; Tada, H.; Aso, Y. *Org. Lett.* **2008**, *10*, 833.

(13) Letizia, J. A.; Salata, M. R.; Tribout, C. M.; Facchetti, A.; Ratner, M. A.; Marks, T. J. *J. Am. Chem. Soc.* **2008**, *130*, 9679.

(14) (a) Winkler, M.; Houk, K. N. *J. Am. Chem. Soc.* **2007**, *129*, 1805. (b) Babel, A.; Jenekhe, S. A. *J. Am. Chem. Soc.* **2003**, *125*, 13656. (c) Nishida, J. I.; Naraso; Murai, S.; Fujiwara, E.; Tada, H.; Tomura, M.; Yamashita, Y. *Org. Lett.* **2004**, *6*, 2007.

(15) Usta, H.; Risko, C.; Wang, Z.; Huang, H.; Deliomeroglu, M. K.; Zhukhovitskiy, A.; Facchetti, A.; Marks, T. J. *J. Am. Chem. Soc.* **2009**, *131*, 5586.

(16) Cai, X. Y.; Burand, M. W.; Newman, C. R.; da Silva, D. A.; Pappenfus, T. M.; Bader, M. M.; Brédas, J. L.; Mann, K. R.; Frisbie, C. D. *J. Phys. Chem. B* **2006**, *110*, 14590.

(17) (a) Jones, B. A.; Facchetti, A.; Wasielewski, M. R.; Marks, T. J. *J. Am. Chem. Soc.* **2007**, *129*, 15259. (b) de Leeuw, D. M.; Simenon, M. M. J.; Brown, A. R.; Einerhand, R. E. F. *Synth. Met.* **1997**, *87*, 53.

(18) Coropceanu, V.; Cornil, J.; da Silva, D. A.; Olivier, Y.; Silber, R.; Brédas, J. L. *Chem. Rev.* **2007**, *107*, 926.

(19) Hutchison, G. R.; Ratner, M. A.; Marks, T. J. *J. Am. Chem. Soc.* **2005**, *127*, 16866.

(20) Liu, H. G.; Kang, S.; Lee, J. Y. *J. Phys. Chem. B* **2011**, *115*, 5113.

(21) Guo, X. G.; Ortiz, R. P.; Zheng, Y.; Hu, Y.; Noh, Y. Y.; Baeg, K. J.; Facchetti, A.; Marks, T. J. *J. Am. Chem. Soc.* **2011**, *133*, 1405.
(22) Ahmed, E.; Earmme, T.; Ren, G. Q.; Jenekhe, S. A. *Chem. Mater.* **2010**, *22*, 5786.
(23) (a) Chua, L. L.; Zaumseil, J.; Chang, J. F.; Ou, E. C. W.; Ho, P. K. H.; Sirringhaus, H.; Friend, R. H. *Nature* **2005**, *434*, 194. (b) Yoon, M. H.; Kim, C.; Facchetti, A.; Marks, T. J. *J. Am. Chem. Soc.* **2006**, *128*, 12851.
(24) (a) Kim, W. S.; Kim, J.; Park, J. K.; Mukamel, S.; Rhee, S. K.; Choi, Y. K.; Lee, J. Y. *J. Phys. Chem. B* **2005**, *109*, 2868. (b) Rathore, R.; Abdelwahed, S. H.; Guzei, I. A. *J. Am. Chem. Soc.* **2003**, *125*, 8712.
(25) Zhan, C. G.; Nichols, J. A.; Dixon, D. A. *J. Phys. Chem. A* **2003**, *107*, 4184.
(26) (a) Rienstra-Kiracofe, J. C.; Tschumper, G. S.; Schaefer, H. F.; Nandi, S.; Ellison, G. B. *Chem. Rev.* **2002**, *102*, 231. (b) Rienstra-Kiracofe, J. C.; Barden, C. J.; Brown, S. T.; Schaefer, H. F. *J. Phys. Chem. A* **2001**, *105*, 524.
(27) Muscat, J.; Wander, A.; Harrison, N. M. *Chem. Phys. Lett.* **2001**, *342*, 397.
(28) Curtiss, L. A.; Redfern, P. C.; Raghavachari, K.; Pople, J. A. *J. Chem. Phys.* **2001**, *114*, 108.
(29) (a) Wu, Q.; Yang, W. *J. Chem. Phys.* **2002**, *116*, 515. (b) Wu, X.; Vargas, M. C.; Nayak, S.; Lotrich, V.; Scoles, G. *J. Chem. Phys.* **2001**, *115*, 8748. (c) Kurita, N.; Sekino, H. *Chem. Phys. Lett.* **2001**, *348*, 139.
(30) (a) Tsuzuki, S.; Uchimaru, T.; Sugawara, K. I.; Mikami, M. *J. Chem. Phys.* **2002**, *117*, 11216. (b) Sinnokrot, M. O.; Valeev, E. F.; Sherrill, C. D. *J. Am. Chem. Soc.* **2002**, *124*, 10887. (c) Tsuzuki, S.; Honda, K.; Uchimaru, T.; Mikami, M.; Tanabe, K. *J. Am. Chem. Soc.* **2002**, *124*, 104.
(31) Suhai, S. *Int. J. Quantum Chem.* **1992**, *42*, 193.
(32) (a) Fabiano, E.; Della Sala, F.; Cingoland, R.; Weimer, M.; Görling, A. *J. Phys. Chem.* **2005**, *109*, 3078. (b) Hutchison, G. R.; Ratner, M. A.; Marks, T. J. *J. Phys. Chem. B* **2005**, *109*, 3126. (c) Hutchison, G. R.; Ratner, M. A.; Marks, T. J. *J. Am. Chem. Soc.* **2005**, *127*, 2339. (d) Hutchison, G. R.; Zhao, Y. J.; Delley, B.; Freeman, A. F.; Ratner, M. A.; Marks, T. J. *Phys. Rev. B* **2003**, *68*, 035204.
(33) (a) Zhao, Y.; Truhlar, D. G. *J. Phys. Chem. A* **2004**, *108*, 6908. (b) Zhao, Y.; Truhlar, D. G. *J. Chem. Theory Comput.* **2005**, *1*, 415.
(34) Dkhissi, A.; Blossey, R. *Chem. Phys. Lett.* **2007**, *439*, 35.
(35) Gil, A.; Branchadell, V.; Bertran, J.; Oliva, A. *J. Phys. Chem. B* **2007**, *111*, 9372.
(36) Curtis, M. D.; Cao, J.; Kampf, J. W. *J. Am. Chem. Soc.* **2004**, *126*, 4318.
(37) Frisch, M. J. et al. Gaussian 03, revision D.02; Gaussian Inc.: Pittsburgh, PA, 2006.
(38) Atkins, P. W. *Physical Chemistry*, 5th ed.; Oxford University Press: Oxford, U.K., 1994.
(39) (a) Marcus, R. A. *Rev. Mod. Phys.* **1993**, *65*, 599. (b) Barbara, P. F.; Meyer, T. J.; Ratner, M. A. *J. Phys. Chem.* **1996**, *100*, 13148. (c) Cornil, J.; Brédas, J. L.; Zaumseil, J.; Sirringhaus, H. *Adv. Mater.* **2007**, *19*, 1791.
(40) Koopmans, T. *Physica* **1934**, *1*, 104.
(41) Valeev, E. F.; Coropceanu, V.; da Silva, D. A.; Salman, S.; Brédas, J. L. *J. Am. Chem. Soc.* **2006**, *128*, 9882.
(42) Löwdin, P. O. *J. Chem. Phys.* **1950**, *18*, 365.
(43) Umemoto, Y.; Le, Y.; Saeki, A.; Seki, S.; Tagawa, S.; Aso, Y. *Org. Lett.* **2008**, *10*, 1095.
(44) (a) Brédas, J. L.; Beljonne, D.; Cornil, J.; Calbert, J. P.; Shuai, Z.; Silbey, R. *Synth. Met.* **2001**, *125*, 107. (b) Cornil, J.; Beljonne, D.; Calbert, J. P.; Brédas, J. L. *Adv. Mater.* **2001**, *13*, 1053. (c) Li, X. C.; Sirringhaus, H.; Garnier, F.; Holmes, A. B.; Moratti, S. C.; Feeder, N.; Clegg, W.; Teat, S. J.; Friend, R. H. *J. Am. Chem. Soc.* **1998**, *120*, 2206.
(45) Pope, M.; Swenberg, C. E. Electronic Processes. In *Organic Crystals and Polymers*, 2nd ed.; Oxford University Press: New York, 1999.
(46) Kulkarni, A. P.; Tonzola, C. J.; Babel, A.; Jenekhe, S. A. *Chem. Mater.* **2004**, *16*, 4556.
(47) Senthilkumar, K.; Grozema, F. C.; Guerra, C. F.; Bickelhaupt, F. M.; Lewis, F. D.; Berlin, Y. A.; Ratner, M. A.; Siebbeles, L. D. A. *J. Am. Chem. Soc.* **2005**, *127*, 14894.
(48) Brédas, J. L.; Calbert, J. P.; da Silva, D. A.; Cornil, J. *Proc. Natl. Acad. Sci. U.S.A.* **2002**, *99*, 5804.
(49) Warta, W.; Karl, N. *Phys. Rev. B* **1985**, *32*, 1172.